CHAPTER IV
NO REDUCTION BY UREA UNDER LEAN CONDITIONS OVER ALUMINA SUPPORTED CATALYSTS *

4.1 Abstract

We prepared Pt on alumina and Au on alumina catalysts using a single step sol-gel process and traditional techniques, such as impregnation and deposition-precipitation. The activity of these catalysts was tested for NO_x reduction with aqueous urea solutions under oxidizing conditions. Our results show that when a bubbler was used to feed urea and water, catalysts prepared by the sol-gel process had better performance than the catalysts prepared with impregnation and deposition-precipitation methods. The NO_x conversion changed almost linearly over Au on alumina catalysts regardless of preparation techniques but over the single step sol-gel synthesized Pt on alumina catalyst (Pt-SG) a typical dome shape of the conversion versus temperature curve was observed. Oxygen in the feed increased the conversion activity and the presence of SO_2 did not have an adverse effect on the activity of Pt-SG and the single step sol-gel Au on alumina (Au-SG) and the impregnation Au on sol-gel alumina (Au-IMP-SG) catalysts.

Keywords: Selective NO reduction, Platinum/alumina catalyst, Gold/alumina, Sol-gel preparation, Urea

4.2 Introduction

Iwamato and Hamada [1], and Hamada et al. [2] showed independently that hydrocarbons could be used as reducing agents to reduce nitrogen oxides in an oxidizing atmosphere; such as the exhaust of a diesel vehicle. Soon after, many

---

* Published manuscript:
Seker, E., Gulari, E., Hammerle, R.H., Lambert, C., Leerat, J., and Osuwan, S. (2002) NO reduction by urea under lean conditions over alumina supported catalysts. Applied Catalysis A: General, 226, 183-192.

possible catalysts for formulations have been extensively studied to find viable catalysts and reductants, which are effective for the selective reduction of NO_x in the exhaust of a lean burn gasoline or a diesel engine. Early studies showed that Pt on alumina, Ag on alumina and Au on alumina catalyst were active in the range of 150-500 ^oC and hydrothermally stable [3-7]. However, each catalyst suffers from either low activity at low temperatures (e.g. less than 200 ^oC) and at high space velocities, such as Ag on alumina, or low N_2 selectivity, such as Pt on alumina [4,6,8,12]. To overcome these disadvantages, different types of hydrocarbons [12,13], oxygenated hydrocarbons [4,5] and also the different preparation methods [7,10,11] were investigated. It has been reported that hydrocarbons and oxygenated hydrocarbons as reductants have been found to have low to moderate reducing efficiency and to result in undesired by-products [13,14]. Also, it was found that sol-gel prepared alumina supported catalysts [10-12] were active at high space velocities and relatively high N_2 selectivity. These investigations have shown that the reduction of NO_x in the exhaust of a diesel vehicle is still challenging due to future air quality standards and low to moderate efficiency of hydrocarbon reductants. In contrast, ammonia has been known to be very selective in the reduction of NO_x from the flue gas streams of power plants. Unfortunately, because of storage and handling difficulties of ammonia and also rapid changing condition of automobile exhaust gas, using ammonia as a reductant for the removal of NO_x from the automobile exhaust gas may not be commercially viable. In contrast of using pure ammonia directly, ammonia can be generated in situ by hydrolysis and decomposition of urea through the following reactions:

$$CO(NH_2)_2 \Longrightarrow NH_3 + HNCO \quad (1)$$

$$HNCO + H_2O \Longrightarrow NH_3 + CO_2 \quad (2)$$

It seems that urea, as ammonia source is the best choice for such applications because urea is not toxic and also can be easily transported on board of an automobile as a high concentration aqueous solution. As a result, NO_x can be reduced not only with ammonia but also the urea itself and its decomposition by-product, HNCO, as shown in reactions (3) – (5):

$$2CO(NH_2)_2 + 6NO \quad ==> \quad 5N_2 + 2CO_2 + 4H_2O \qquad (3)$$

$$4HNCO + 6NO \quad ==> \quad 5N_2 + 4CO_2 + 2H_2O \qquad (4)$$

$$4NH_3 + 4NO + O_2 \quad ==> \quad 4N_2 + 6H_2O \qquad (5)$$

Even though the use of urea in the reduction of NO_x from the flue gas streams of power plants is a well established method [15], there are not many studies on the application of using urea as a reductant in the treatment of the lean burn engine operated vehicles.

Held et al. [16] showed the applicability of urea as the reductant in reducing the NO_x from the diesel engine exhaust with the Cu/ZSM-5 catalyst but their study also raised several questions, such as urea dosage control, that need to be resolved. V_2O_5-based catalysts were studied for the redution of NO_x by urea in real diesel exhaust gas [18,19]. However, for automotive applications use of highly toxic vanadia-based catalysts pose some serious health problems, such as high vapor pressure of the oxide leading to toxic emissions and the potential for water solubility and leaching of the oxide from cold catalyst beds by condensing water vapor [20]. Fundamental studies on hydrolysis and decompostion of urea in the gas phase or over a catalytic material have been performed to understand the individual steps involved in the reduction of NO_x by urea [17-19]. Despite these studies no single catalyst has been identified as being effective at low temperatures for both urea hydrolysis/decomposition and NO reduction.

In this paper, we report the catalytic activities of Pt on alumina and Au on alumina catalysts for NO reduction by urea in an oxidizing atmosphere. We introduced urea into the feed gas by using a bubbler to study the relationship between catalytic activity and the effect of gas phase composition on the activity and N_2 selectivity. We also studied the catalytic activities as a function of catalyst preparation method: sol-gel, impregnation and depositon-precipitation methods.

4.3 Experimental

4.3.1 Catalyst Preparations and Activation

Aluminum tri-*sec*-butoxide was used to make alumina supported Pt or Au catalyst and pure alumina material. Chloroplatinic acid and gold acetate were the metal precursors for Pt loading and Au loading, respectively. Single step sol-gel supported catalysts were prepared in the same way as in [9]. Aluminum tri-*sec*-butoxide was first mixed with the water-ethanol solution and then the necessary amount of chloroplatinic acid or gold acetate was added to the alumina sol solution. The resulting gel was dried at 100 °C for 12 h to remove the solvent and water. Then, it was calcined at 600 °C for 24 h prior to activity studies.

For impregnation catalyst, we synthesized alumina by the same sol-gel method as reported in [9]. The sol-gel made alumina was also dried at 100 °C for 12 h and calcined in air at 600 °C for 24 h. For Au loading, we used hydrogen tetrachloroaurate to make impregnation Au on the sol-gel alumina. Impregnated alumina support was dried at 100 °C for 5 h and calcined at 500 °C for 5 h.

The deposition-precipitation method described in [7] was used to prepare the Au on alumina with hydrogen tetrachloroaurate precursor. We used two different alumina supports; and alumina obtained from Aldrich Inc. (γ-alumina with 150 m^2/g) and the alumina we synthesized by the same sol-gel method given as in [9]. The deposition-precipitation catalyst was dried at 100 °C for 5 h and calcined at 500 °C for 5 h prior to activity studies.

We activated all catalysts with a gas mixture containing 750 ppm NO, 750 ppm propene, 7% oxygen, ~2% water and He as balance. The total flow rate of 75 ml/min was passed over 0.1 g of the catalyst and the catalyst was subjected to a temperature ramp from 150 to 500 °C with a 50 °C step increment. Once 500 °C was reached, they were kept at this temperature overnight. After being used under this reaction cycle for several times, all catalysts reached their stable activity levels. We noticed that the color of the single step sol-gel Au on alumina catalyst changed from light pink to purple at the end of activation cycle. The color change was not observed for other Au on alumina catalysts made with the impregnation and deposition-precipitation methods.

4.3.2 Catalyst Testing

The calcined catalysts were ground and sieved to 80-120 mesh size prior to activity tests. In all experiments, we tested 0.1 g of catalyst, held between two quartz wool plugs in a quartz U tube (i.d. 3 mm.) flow reactor, under a total flow rate of 177 ml/min. The reactant gas mixture was blended by using four independent mass flow controllers to give 750 ppm NO (with ~20 ppm NO_2 comes from NO cylinder), 0-14% O_2, 25 ppm SO_2 (when used) and He as balance. NO, O_2 and He streams were mixed together before entering to the bubbler containing aqueous urea solution. SO_2 (when used) was added to the outlet stream of the bubbler to prevent the absorption of SO_2 in the bubbler before total feed stream entered to the heated section of the U tube reactor.

Varying amounts of urea (Aldrich) was dissolved in 50 ml of water. Then, this solution was transferred to a glass bubbler kept at room temperature. The feed gas mixture, containing NO, O_2 and He, was passed through this bubbler to strip-off urea and water into the gas phase.

The reactor outlet stream passed through a membrane dryer (from Perma Pure Inc.) to remove water and phosphoric acid trap to eliminate NH_3 and HNCO from the reactor outlet stream. Then, it was analyzed by using a Thermo Environmental 42CHL NO_x Chemiluminescence Analyzer to determine unreacted NO_x and also a FT-IR with a 10 cm path length gas cell for quantitative determination of CO_2, CO and N_2O. A GC equipped with TCD detector (from SRI Inc.) was used to analyze NH_3. For NH_3 analysis, we used a 6 ft long Porapak N column (from Alltech Inc.) operated isothermally at 80 ^oC and also we double-checked the concentration of ammonia at the outlet by using an ammonia analysis kit after absorbing it in water at 0 ^oC. The activity measurements were reproducible within ±2% and the N_2O selectivity measurements were accurate to ~5 ppm resulting in an error bar of ±2% in N_2 selectivity at 50% NO_x conversion.

4.3.3 Catalyst Characterization

Approximate crystallite size and phases present in the catalysts were determined by X-ray diffraction (Rigaku powder diffractometer, operated at 40 kV

and 100 mA). BET surface area was measured with a Micromeritics 2010 instrument. Prior to analysis, the sample was degassed under vacuum at 300 until the vacuum inside the sample tube stayed constant at around 5 μmHg. A standard Micromeritics program was employed to calculate both BET surface area and BJH pore size distribution (using the desorption isotherm).

JEOL 4000 HRTEM was also used to determine Pt and Au particle sizes and their distribution in the single step sol-gel synthesized Pt on alumina catalyst and the single step sol-gel Au on alumina (fresh and activated ones). Catalyst powder was ground in *i*-propyl alcohol and then kept in a sonic bath for 15 min. A drop of the alcohol powder suspension was put on a holly carbon-coated copper screen and then alcohol was evaporated at room temperature under vacuum before transferring to HRTEM column. An amount of 90-200 crystallite pictures for each catalyst were collected spatially over holly carbon coated copper screen to find the crystallite size distribution for Pt and Au.

The neutron activation analysis technique was performed at the Ford Nuclear Reactor at the University of Michigan to find the gold amount in the single step sol-gel Au on alumina and the deposition-precipitation Au on sol-gel alumina catalysts. The concentration of gold in aluminum matrix was determined through direct comparison to the standard reference material NBS-SRM-2128-1 (1 ± 0.01% Au). Approximately 100 mg of the liquid standard was placed on thin strips of filter paper in polyethylene vials, the mass recorded to the nearest 0.1 mg, and the standards dried to constant weight. Similarly, approximately 10 mg of the sample material was similarly prepared. Samples and standards were irradiated in position L70D (with an average thermal neutron flux of ca. 3.9×10^{11}) for 1 h; samples were rotated during irradiation to ensure equal exposure to neutron flux. Following irradiation, the resulting gamma activity in each vial was counted using a high purity germanium (HPGe) detector, for 5,000 s, resulting in peak areas with associated errors of less than 1%. Gold concentrations in the unknowns were based on the decay-corrected gamma activity per milligram averaged across four standards, while a fifth replicate served as a check standard for quality control. The check standard indicated a total measurement error of ca. 0.04%.

4.4 Results and Discussion

4.4.1 Results

4.4.1.1 Metal Amount in All Catalysts

The analysis of the single step sol-gel synthesized Pt on alumina catalyst (designated as Pt-SG) with ICP analysis showed that Pt loading was 2 wt%. Also, the analysis of Au content in the single step sol-gel Au on alumina catalyst (designated as Au-SG) and the deposition–precipitation Au on the sol-gel alumina catalyst (designated as Au-DP-SG) with the neutron activation analysis technique was found to be 0.7 and ~0.55 wt%, respectively. Au loading in the impregnation Au on the sol-gel alumina catalyst (designated as Au-IMP-SG) was ~0.75 wt% (based on the weight of gold precursor measured to the nearest 0.1 mg with a balance). The deposition-precipitation Au on the commercial alumina (designated as Au-DP-gamma) catalyst was assumed to have ~0.6 wt% gold loading since it was made under the same preparation condition and the same amount of gold precursor used to make Au-DP-SG catalyst.

4.4.1.2 Catalyst Characterization

XRD spectrum for the Pt-SG catalyst showed Pt peaks at 2θ of ~40, ~46, and ~67.5° superimposed on alumina peaks (γ and η) at 2θ of ~39, ~45.5 and ~66.8°. Approximate Pt crystallite size obtained by the Debye-Scherrer equation using the Pt(1 1 1) peak is 16 ± 1 nm. Because of the sensitivity of XRD analysis, only to crystallites larger than 5 nm, we also used HRTEM to determine the average crystallite sizes distribution of the Pt-SG catalyst based on a sample of 200 Pt crystallite pictures. The distribution appeared to have two very close peaks with 34% of the crystallites counted having a size of 13 ± 2 nm and 16% having a size of 20 ± 7 nm. The arithmetic average of this distribution is 15.5 ± 6 nm in excellent agreement with the XRD results.

XRD spectra of Au-SG and Au-IMP-SG catalysts showed Au peaks at ~38, ~44.5, and ~64.5° 2θ superimposed on alumina peaks at ~39, ~45.5, and ~66.8° 2θ and also two more gold peaks at ~77.5 and ~81.5° 2θ without any interference from the alumina phase. Analysis of the XRD pattern for our alumina

support for these catalysts showed γ-alumina. The approximate gold crystallite sizes of fresh catalysts were also obtained using the Debye-Scherrer equation and the Au(1 1 1) peak. The average gold crystallite sizes for Au-SG and Au-IMP-SG were found to be the same, ~34 nm. XRD measurements for Au-DP-SG and Au-DP-gamma did not reveal any detectable Au crystallites. Because of the small amount of catalyst used during the reduction reaction, we could not use XRD to measure the average Au particle size of activated Au-SG catalyst (purple). However, we used HRTEM to determine the Au particle size distribution of the activated Au-SG (purple) and the fresh Au-SG (light pink) based on the 90 Au crystallite pictures. We found out that the activated Au-SG (purple) and the fresh Au-SG (light pink) had a crystallite size of D ~9 ± 3 and ~37 ± 10 nm, respectively. This shows that Au crystallites in the fresh Au-SG catalyst (light pink) redispersed under the reaction condition, hence resulting in a more active catalyst and smaller crystallites. The sol-gel synthesis and calcination treatment we use produces Pt-SG catalyst with BET suface area of ~300 m^2/g and a narrow pore size distribution centered at D ~68 Å. In contrast, when alumina is synthesized alone there is no change in surface area but the average pore size becomes ~77 Å. In comparison, the surface area of the commercial (Aldrich) γ-alumina is 150 m^2/g. BET surface area of Au-SG is ~250 m^2/g and its pore size distribution is bimodal. Approximately 15% of the pores centered at D ~35 ± 7 Å and the rest centered at ~90 ± 20 Å. All pores of this catalyst are below 150 Å.

4.4.1.3 NO_x Reduction by Urea

Originally, we did not have a pump with a low enough volumetric flow rate to inject the urea solution into the feed stream and decided to try bubbling the feed gasses through an aqueous solution of urea. Interestingly, we observed that urea in this aqueous solution could be carried into the gas phase by the feed gas. The presence of urea in the gas phase was confirmed with the measurement of CO_2 at the outlet of the reactor. The formation of CO_2 can only happen when urea is decomposed and hydrolyzed, hence proving that urea was carried to the reactor with the feed gas stream.

In order to understand how urea is stripped off from the solution to the gas phase, we conducted three sets of experiments. First, we examined

to see if urea decomposes or hydrolyzes in the gas phase. For this experiment, we did not use a catalyst, i.e. just empty quartz U tube. The feed gas of 750 ppm NO and 7% oxygen in helium was bubbled through aqueous urea solution. Then, we measured the steady-state gas phase activity from 150 to 500 °C with a 50 °C step increment. We found out that in this temperature range, there was neither CO_2 or NH_3 formation nor NO_x conversion. Also, the measurement of NO concentration in the feed before and after the bubbler showed that NO did not absorb in aqueous urea solution throughout the experiment. However, in the presence of a catalyst, e.g. Pt-SG catalyst, we observed the formation of CO_2 and NO_x conversion under the same reaction conditions. Secondly, over the Pt-SG catalyst, we investigated if there is a relationship between the amount of urea carried into the gas phase and the feed gas composition. We changed the NO concentration in the feed from 750 to 0 ppm but we kept oxygen concentration at 14% and found out that in the absence of NO in the feed, there was no CO_2 or NH_3 formation. This indicates that urea was not present in the gas phase. However, CO_2 formation was observed as soon as NO was introduced into the feed. In fact, the amount of CO_2 formation for a constant urea concentration in the bubbler increased as a function of NO concentration in the feed and temperature as seen in Figure 4.1 (a). In all runs, NH_3 concentration at the reactor outlet was less than 2 ppm at all temperatures, as seen in Figure 4.1 (b). Finally, we changed the amount of urea in the aqueous urea solution but kept the feed gas concentration constant. We used 0.3 and 0.7 g urea dissolved in 50 ml of water while keeping the feed gas composition constant (750 ppm NO and 7% O_2 in He). With both urea concentrations, we observed that there was no change in the NO conversion as a function of temperature. As a result, we concluded that urea can be stripped off from the solution to gas phase only in the presence of NO in the feed and that the amount of urea carried to gas phase is not dependent on the urea amount in the aqueous urea solution and the decomposition and hydrolysis of urea over Pt-SG is strongly dependent on the temperature.

We further investigated the effect of reaction conditions, such as varying oxygen and SO_2 concentration, on the catalytic activity of Pt-SG. Figure 4.2 shows that the NO_x conversion activity of Pt-SG as a function of oxygen concentration. The aqueous urea concentration and NO_x concentration were kept

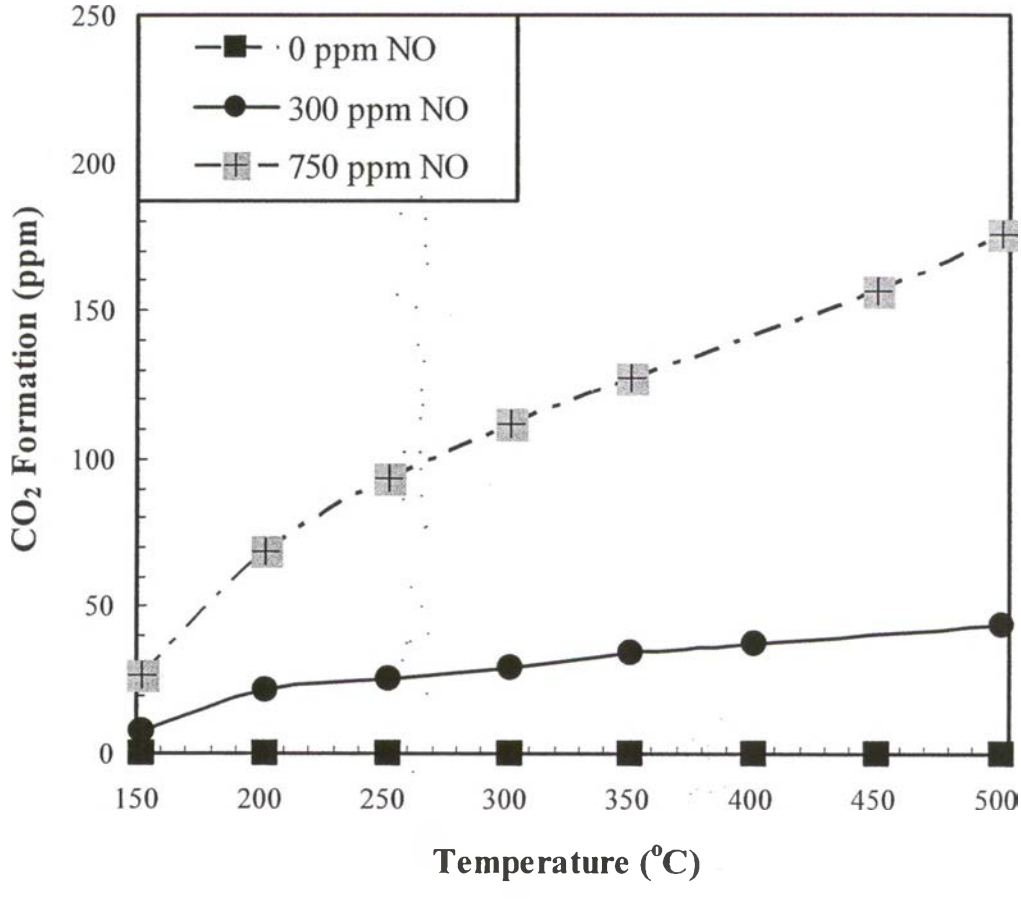

Figure 4.1 (a) The catalytic activity of the Pt-SG catalyst as a function of NO concentration. Reaction conditions: above NO concentrations, 14% oxygen and 1.4 wt% aqueous urea solution, 0.1 g catalyst and 177 ml/min of total dry gas flow rate.

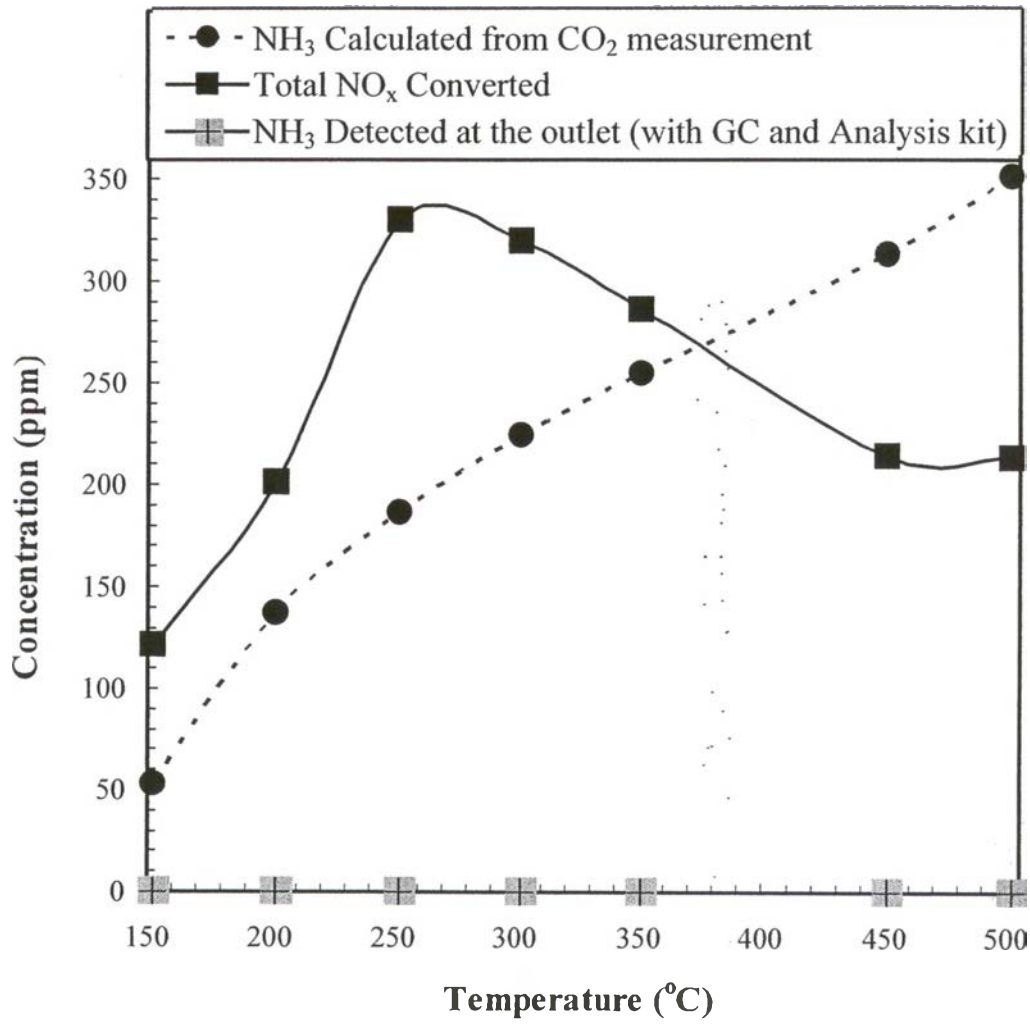

Figure 4.1 (b) The catalytic activity of the Pt-SG catalyst. Reaction conditions: 750 ppm NO concentrations, 14% oxygen and 1.4 wt% aqueous urea solution, 0.1 g catalyst and 177 ml/min of total dry gas flow rate.

constant at 1.4 wt% and 750 ppm, respectively, and the oxygen concentration was varied from 0 to 14%. As seen in Figure 4.2, in the absence of oxygen, the catalyst shows only very low level of activity above 400 °C and reaches its maximum NO_x conversion, ~5%, at 500 °C. On the other hand, when O_2 in the feed is 7.5%, ~6% conversion is obtained at 150 °C and the NO_x conversion reaches its maximum, ~36%, at 250 °C, then slowly decreases to 16% at 500 °C. Increasing O_2 concentration further to 14% results in higher conversions at all temperatures. The maximum NO_x conversion, ~45%, is also obtained at 250 °C and with conversions at 150 and 500 °C being ~19 and ~25%, respectively.

We observed that over the Pt-SG catalyst, in the absence of oxygen, a very low amount of CO_2 is formed above 400 °C but the CO_2 amount increases as a function of oxygen and temperature. This indicates that hydrolysis of urea under our reaction condition does not occur over Pt-SG without oxygen. However, it is probable that urea decomposes directly into NH_3 and HNCO. Figure 4.3 shows the effect of 25 ppm SO_2 on the NO_x conversion activity of Pt-SG. As can be seen in Figure 4.3, at 300 °C, NO_x conversions obtained with SO_2 and without SO_2 in the feed are similar. On the other hand, above 300 °C, we see that NO_x conversion activity of the catalyst is slightly enhanced. For example, at 500 °C, ~37% conversion is obtained in the presence of SO_2 in the feed while the conversion in the absence of SO_2 in the feed is ~29%. Above 250 °C, the CO_2 amount formed during the reduction reaction in the presence of 25 ppm SO_2 in the feed is higher than that obtained without SO_2. However, below 250 °C, CO_2 amounts with and without SO_2 in the feed are similar within our experimental error.

As comparison to Pt-SG catalyst, we also studied NO reduction with urea over Au/alumina catalysts by using the bubbler. Figure 4.4 shows the activity of Au-SG as a function of oxygen concentration. Similar to Pt-SG catalyst, NO_x conversion increases with oxygen concentration at all temperatures. Interestingly, the conversion over Au-SG increases almost linearly with temperature. When oxygen concentration in the feed is 14%, the conversion increases from ~30% at 150 °C to ~60% at 500 °C. When we included 25 ppm SO_2 in the feed with 750 ppm NO, 14% O_2, there was no detectable effect of SO_2 on the NO_x reduction activity of Au-SG catalyst over the whole temperature range. Similarly, the amount

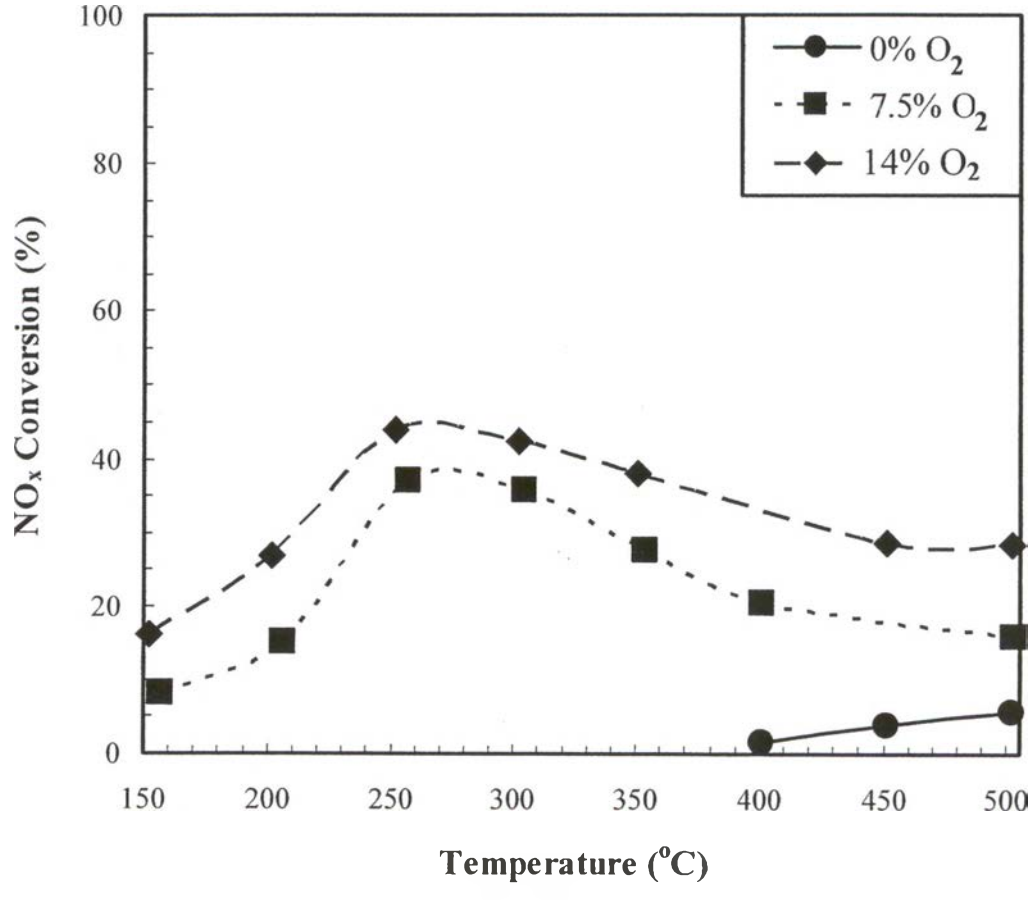

Figure 4.2 The activity of Pt-SG catalyst as a function of oxygen concentration. Reaction condition: 750 ppm NO and above oxygen concentrations and 1.4 wt% aqueous urea solution, 0.1 g of catalyst and 177 ml/min of total dry gas flow rate.

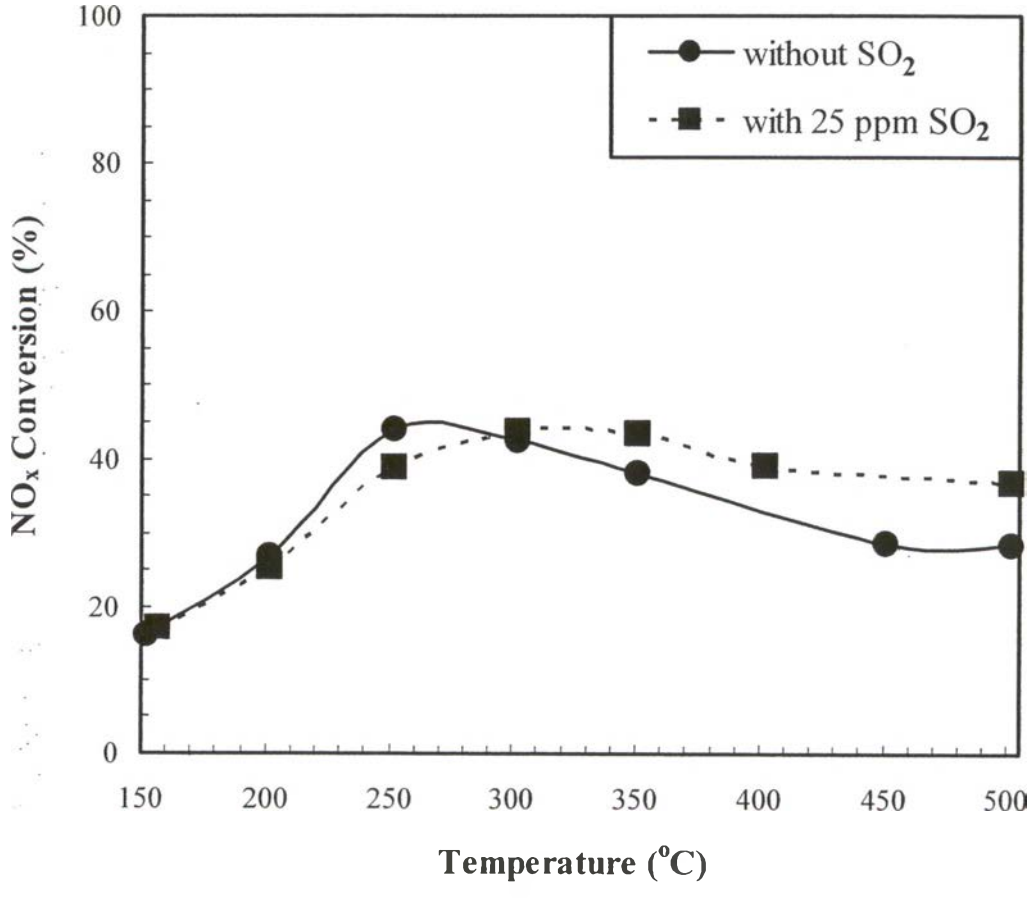

Figure 4.3 Effect of SO_2 concentration on the activity of Pt-SG catalyst. Reaction conditions: 750 ppm NO, 14% oxygen and 1.4 wt% aqueous urea solution, 0.1 g of catalyst and 177 ml/min of total dry gas flow rate.

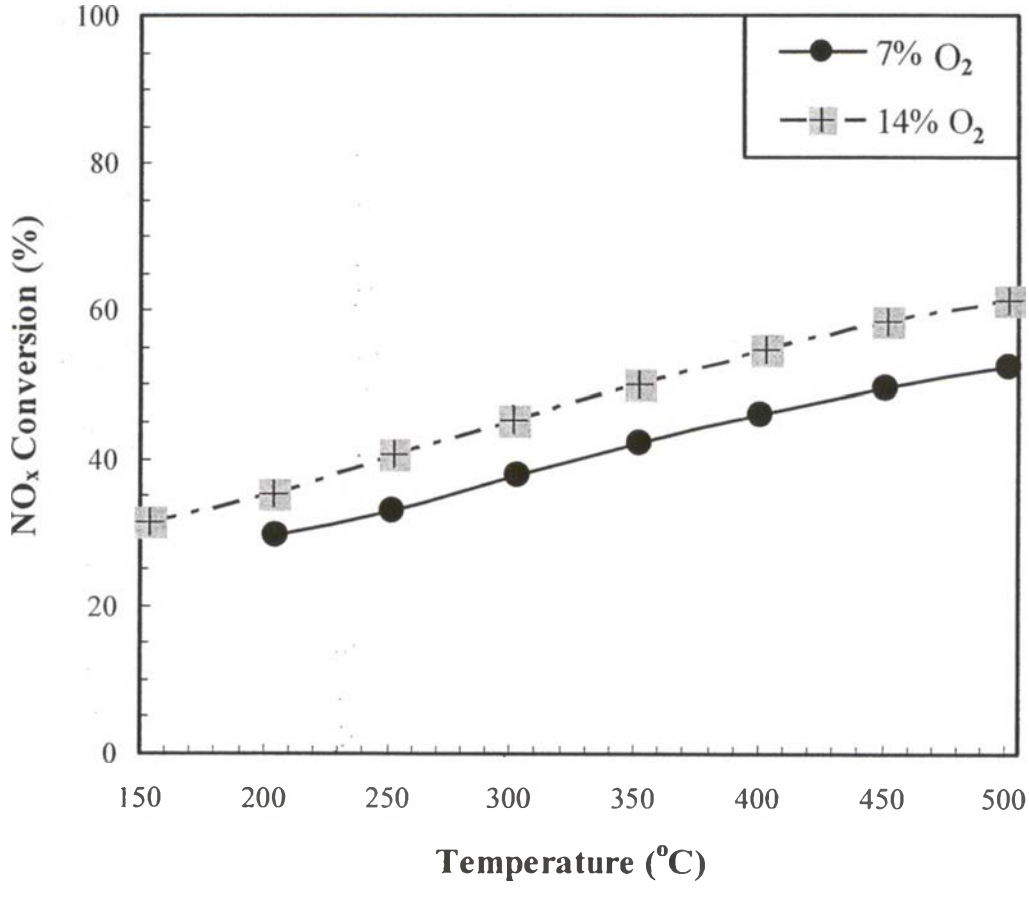

Figure 4.4 Effect of O_2 concentration on the activity of Au-SG catalyst. Reaction conditions: 1,000 ppm NO, above oxygen concentrations and 1.4 wt% aqueous urea solution, 0.1 g of catalyst and 177 ml/min of total dry gas flow rate.

of CO_2 produced at all temperatures did not change with SO_2 in the feed, as shown in Figure 4.5.

Figure 4.6 shows the effect of the alumina and the preparation method on the NO_x conversion activity of Au on alumina catalysts as a function of temperature. We used two alumina materials in the deposition-precipitation method. One was prepared in our laboratory by using our sol-gel procedure and the other one was obtained from Aldrich Inc. After calcination, all catalysts were activated and were tested with the reaction mixture of 750 ppm NO and 7% O_2. As seen in Figure 4.6, Au-IMP-SG and Au-DP-gamma catalysts show very low conversions for all temperatures. However, the deposition-precipitation catalyst (Au-DP-SG), made using our sol-gel alumina, is very active and its activity is similar to that of Au-SG catalyst. This shows that not only the preparation method but also the support material is crucial to get active Au on alumina catalysts.

4.4.2 Discussion

4.4.2.1 Pt on Alumina Catalyst

The role of oxygen in the NO reduction reaction is seen from the Figure 4.2 In the absence of oxygen, there is no CO_2 formation until 400 °C. This shows that the hydrolysis of HNCO with water does not occur until 400 °C even though the decomposition of urea to ammonia and HNCO may be occurring between 150 and 500 °C. In this case, one may expect to see NO_x reduction by NH_3 and/or HNCO. However, our results do not show any NO_x conversion until 400 °C in the absence of oxygen. Katona et al. (1992) reported that over polycrystalline platinum, NO was reduced by ammonia at very high rate in the presence of oxygen [21]. In addition, Ramis et al. (1995) [22] showed that oxy-dehydrogenation of NH_3, leading to adsorbed NH_2 and H, was the first possible step in the reduction of NO with NH_3 in the presence of oxygen. Studies on the reduction of NO with cyanuric acid or ammonia or isocyanic acid in the gas phase showed that the species, such as H and OH, are the result of oxy-dehydrogenation of NH_3 and H_2O. Also, the presence of these species leads to many parallel reactions in addition to NO reduction to N_2 or N_2O [23,24]. We can speculate that adsorbed oxygen on Pt crystallites reacts with

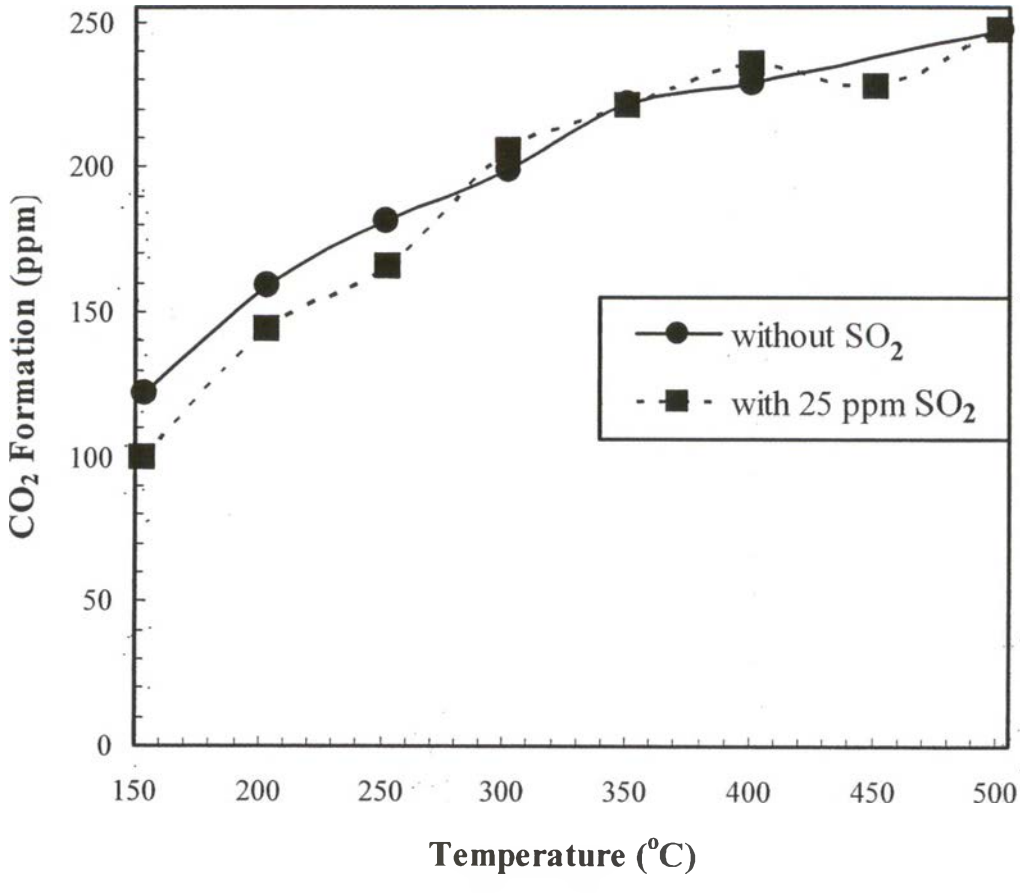

Figure 4.5 Effect of SO_2 concentration on the activity of Au-SG catalyst. Reaction conditions: 750 ppm NO, 14% oxygen and 1.4 wt% aqueous urea solution and above SO_2 concentrations, 0.1 g of catalyst and 177 ml/min of total dry gas flow rate.

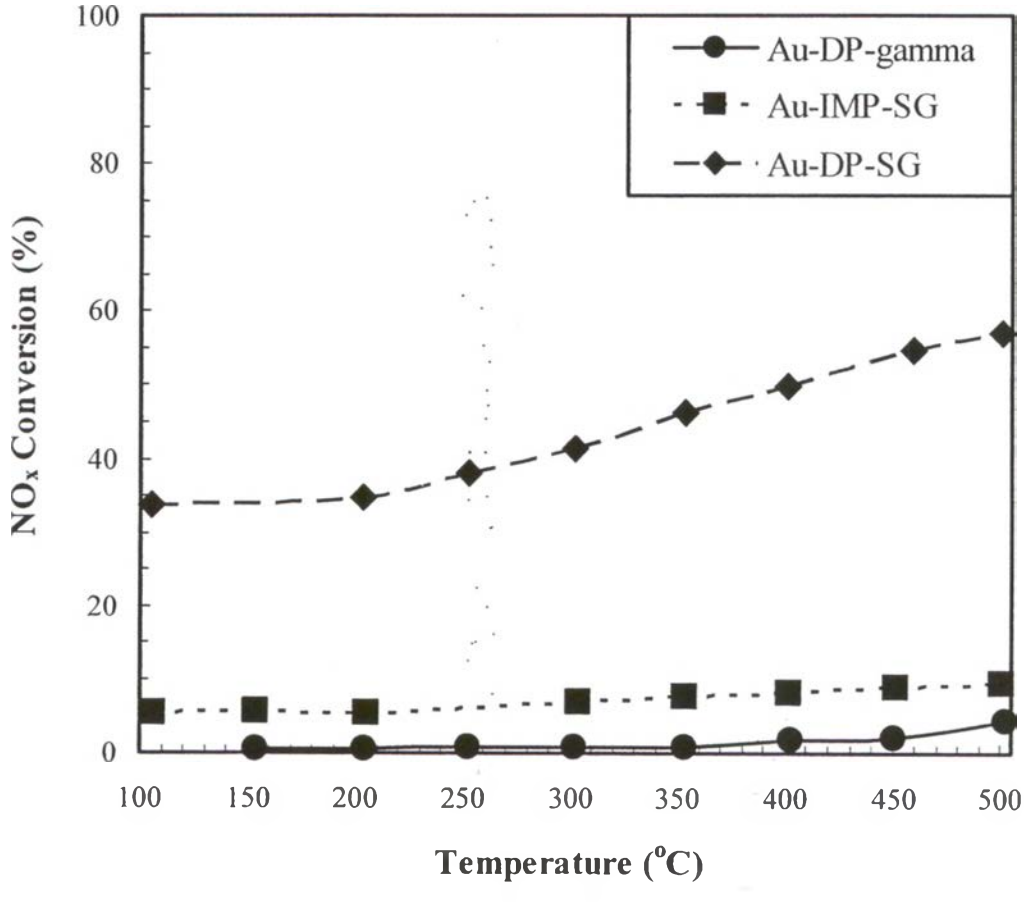

Figure 4.6 Comparison of the activity of Au on alumina catalysts as a function of preparation method and the kind of alumina. Reaction conditions: 750 ppm NO, 7% oxygen and 1.4 wt% aqueous urea solution, 0.1 g of catalyst and 177 ml/min of total dry gas flow rate.

either NH_3 or HNCO to initiate the formation of NH_2 or NH. These ad species reduce NO to N_2 or N_2O.

As seen in Figure 4.1, CO_2 formation increases with the temperature. Our mass balance calculations showed that until 300 °C, 1 mol of CO_2 formation leads to 3 mol of NO converted indicating 100% efficiency in the use of urea. Above 300 °C, we see that NO_x conversion decreases but CO_2 formation increases. This indicates that in the presence of oxygen and water, the hydrolysis and/or oxidation of HNCO increase at high temperatures over the Pt-SG catalyst. This may result in the formation of NO or NO_2 and CO_2 and H_2O. We could not detect any NH_3 at all temperatures in the reactor outlet stream by using the GC and the NH_3 analysis kit. This may be due to the fast oxidation of NH_3 to NO or NO_2 over the catalyst. Hence, the overall conversion of NO_x decreases as the temperature is raised. This also indicates that at low temperatures, some unreacted urea in the gas phase comes out of the reactor. We observed some white precipitate in the inlet and outlet of the reactor tube at the end of the experiment. Koebel et al. (1996) [17] also found unreacted urea at low temperatures coming out of the reactor. At this point, we do not have any information on how much urea is not used in the reaction. We will report the analysis of the reactor outlet in near future [26].

4.4.2.2 Au on Alumina Catalysts

Over the Au-SG and Au-DP-SG catalysts, we observed that NO_x conversion increases almost linearly with the temperature. However, the conversion activity of Au-IMP-SG catalyst is very low. We found that the average gold particle size on Au-SG and Au-DP-SG is ~9 nm (obtained with HRTEM) and less than 5 nm (obtained with XRD), respectively. In contrast, the average gold particle size on Au-IMP-SG catalyst (based on XRD) is ~34 nm. It is known that the gold dispersion and the interface between gold particles and oxide supports might be the important factors in getting active supported gold catalysts, [7,25]. Au-SG and Au-DP-SG catalysts, with small Au crystallites, seem to be very active for the decomposition of urea to NH_3 and HNCO and also possibly for the oxy-dehydrogenation of NH_3. However, the oxidation of N containing species, such as HNCO or NH_3, in addition to NO_x reduction may proceed so slowly that the overall NO_x conversion increases with temperature unlike the Pt-SG catalyst. In fact, we

found that when NH_3 instead of urea was used as a reductant in the presence of oxygen and water, NO_x reduction over Au-DP-SG catalyst was observed until 500 °C. Whereas, NO_x conversion over Pt-SG catalyst became negative between 300 and 500 °C, hence showing that NH_3 was oxidized to NO or NO_2 instead of being used in the reduction of NO. Detailed studies on the reduction of NO with NH_3 over Au on alumina and Pt on alumina catalysts are in progress.

The average Au particle size is around 5 nm for the deposition-precipitation catalysts prepared with the sol-gel alumina (Au-DP-SG) and the commercial alumina (Au-DP-gamma) but their activities for NO reduction with aqueous urea are very different. This could be explained based on the nature of alumina materials. We found that without Au or Pt, our sol-gel made alumina showed higher NO_x conversion than the commercial alumina as seen in Figure 4.7. Even though the NO conversion over sol-gel alumina is low, we observed CO_2 formation at all temperatures. This indicates that alumina itself contributes to the NO reduction and the urea hydrolysis. However, the commercial alumina showed relatively low activity for NO reduction and urea hydrolysis between 200 and 500 °C.

4.4.2.3 SO_2 Effect

The increased conversion observed over the Pt-SG catalyst (as seen in Figure 4.3) in the presence of SO_2 above 300 °C may be due to the formation of metal sulfates at the catalyst surface. Indeed, Pt-SG first oxidizes SO_2 to SO_3, which then leads to the formation sulfates. It is known that the metal sulfates are acidic materials and the hydrolysis of urea is accelerated over acidic materials [17]. Increased hydrolysis rate can lead to increase in NO conversion at high temperatures. However, this activity enhancement is not observed over the Au-SG catalyst. This may be because of low rate of oxidation of SO_2 and metal sulfate formation over the Au-SG catalyst. As can be seen in Figure 4.5, CO_2 amount formed in the presence of SO_2 and in the absence of SO_2 in the feed over the Au-SG catalyst is identical within our experimental measurement error. Also, we did not observe any difference in the NO_x conversion over the Au-SG catalyst in the absence and the presence of SO_2 in the feed.

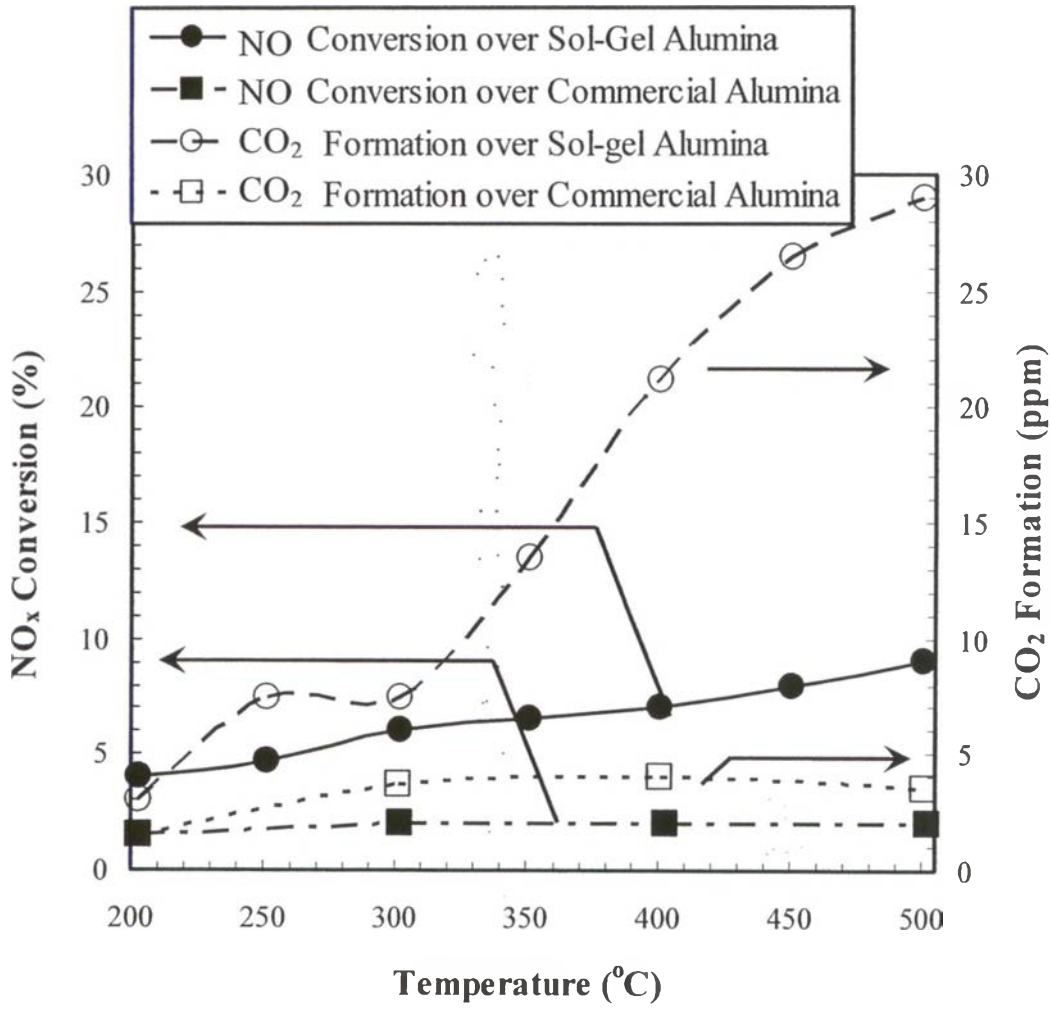

Figure 4.7 Comparison of the activities of sol-gel alumina and the commercial alumina. Reaction conditions: 750 ppm NO, 7% oxygen and 1.4 wt% aqueous urea solution, 0.1 g of catalyst and 177 ml/min of total dry gas flow rate.

4.5 Conclusions

- When the feed is bubbled through a urea solution, urea is carried to the reactor with the feed stream if NO is present. Also, NO measurements before and after the bubbler shows that NO does not absorb in aqueous urea solution.
- High oxygen concentration in the feed is beneficial to get higher NO conversion for all temperatures when the bubbler is used. Also N_2O is not produced for all oxygen concentrations.
- NH_3 slip over all catalysts was less than 2 ppm at all temperatures.
- SO_2 actually enhances the NO conversion above 300 ^oC over Pt-SG but it does not change the conversion temperature curve over Au-SG catalyst. It also does not change N_2 selectivity, ~100% (based on N_2O measurement with FT-IR).
- Au-DP-SG catalyst is very active for NO reduction with urea as compared to the Au-DP-gamma alumina catalyst; hence, indicating the effect of the kind of alumina material for the similar average Au particle size.
- In the absence of O_2, NO_x conversion and urea usage does not occur below 400 ^oC over all catalysts.

4.6 Acknowledgements

Partial Financial support of this research by Ford Motor Company and NSF is gratefully acknowledged. We are also grateful to the Thailand Research Fund for the partial financial support for Ms. Jiraporn Leerat.

4.7 References

[1] M. Iwamato, H. Hamada, Catal. Today 10 (1991) 57-71.

[2] H. Hamada, Y. Kintaichi, M. Sasaki, T. Ito, M. Tabata, Appl. Catal. 75 (1991) L1-L8.

[3] R. Burch, P.J. Millington, A.P. Walker, Appl. Catal. B: Environ. 4 (1994) 65-94.

[4] T. Miyadera, Appl. Catal. B: Environ. 2 (1993) 199-205.

[5] T.E. Hoost, R.J. Kudla, K.M. Collins, M.S. Chattha, Appl. Catal. B: Environ. 13 (1997) 59-67.

[6] K.A. Bethke, H.H. Kung, J. Catal. 172 (1997) 93-102.

[7] A. Ueda, T. Oshima, M. Haruta, Appl. Catal. B: Environ. 12 (1997) 81-93.

[8] R. Burch, T.C. Watling, Appl. Catal. B: Environ. 11 (1997) 207-216.

[9] E. Seker, Ph.D. Thesis, The University of Michigan, Ann Arbor, Michigan, 2000, p. 25.

[10] E. Seker, E. Gulari, J. Catal. 194 (2000) 4-13.

[11] E. Seker, J. Cavataio, E. Gulari, P. Lorpongpaiboon, S. Osuwan, Appl. Catal. A: Gen. 183 (1999) 121-134.

[12] H.W. Jen, Catal. Today 42 (1998) 37-44.

[13] R. Burch, D. Ottery, Appl. Catal. B: Environ. 13 (1997) 105-111.

[14] J.C. Kramlich, W.P. Linak, Prog. Energy Combust. Sci. 20 (1994) 149-202.

[15] H.T. Hug, A. Mayer, A. Hartenstein, SAE Technical Paper Series, 930363, Detriot, 1-5 March 1993.

[16] W. Held, A. König, T. Richter, L. Puppe, SAE Paper, 900496.

[17] M. Koebel, M. Elsener, T. Marti, Combust. Sci. Tech. 121 (1996) 85-102.

[18] M. Koebel, M. Elsner, G. Madia, Ind. Eng. Chem. Res. 40 (2001) 52-59.

[19] T. Morimune, H. Yamaguchi, Y. Yasukawa, Exp. Thermal Fluid Sci. 18 (1998) 220-230.

[20] Reade Advanced Materials, www.reade.com/Products/Oxides/vanadium_oxide.html.

[21] T. Katona, L. Guczi, G.A. Somorjai, J. Catal. 135 (1992) 434-443.

[22] G. Ramis, L. Yi, G. Busca, M. Turco, E. Kotur, R.J. Willey, J. Catal. 157 (1995) 523-535.

[23] J.A. Miller, C.T. Bowman, Int. J. Chem. Kinet. 23 (1991) 289-313.

[24] J.A. Caton, D.L. Siebers, Combust. Sci. Tech. 65 (1989) 277-293.

[25] M. Haruta, S. Tsubota, T. Kobayashi, H. Kageyama, M.J. Genet, B. Delmon, J. Catal. 144 (1993) 175-192.

[26] E. Seker, E. Gulari, C. Lambert, R.H. Hammerle, in preparation.